Discover Nano

Research

Development of essential oils inclusion complexes: a nanotechnology approach with enhanced thermal and light stability

Fernanda Ramalho Procopio[1] · Ramon Peres Brexó[1] · Luis Eduardo Sousa Vitolano[1] · Maria Eduarda da Mata Martins[2] · Maria Eduarda de Almeida Astolfo[3] · Stanislau Bogusz Junior[3] · Marcos David Ferreira[1]

Received: 15 April 2024 / Accepted: 28 November 2024
Published online: 08 December 2024

Abstract
Essential oils (EOs) are volatile compounds that may have antimicrobial and antioxidant properties. Despite their potential application, low water solubility and chemical instability are limiting factors. Nanoencapsulation processes can overcome this problem, protecting against external factors and promoting a moderate release. Therefore, the objective of the present study was to encapsulate *Cymbopogon citratus* (CC) and *Origanum vulgare* (OV) essential oils in β-cyclodextrin (βCD) complexes. Different ratios (w/w) between βCD and EOs (96:4, 92:8, 90:10, 88:12) were tested, seeking greater entrapment efficiency. The particles were characterized by yield, entrapment efficiency, size distribution, morphology, crystallinity, infrared spectroscopy, and thermal behavior. Furthermore, the thermal (70 °C) and photochemical (UV) stability of the free and encapsulated EO was evaluated for 48 h. The results showed that the βCD-CC 90:10 and βCD-OV 90:10 formulations presented greater entrapment efficiency. Crystalline structures of varying sizes (200 to 800 nm), trapezoidal shape, and tendency to aggregation were obtained. Changes in the βCD crystalline organization and the suppression of characteristic free oil absorption bands suggest the EO entrapment. Regarding stability results, βCD-CC remained constant when CC showed losses of 20% (photodegradation) and 60% (thermal degradation) after 48 h of stress exposure. Free OV showed slight variations in absorbance over time, while βCD-OV remained constant over 24 h (thermal degradation) and maintained 60% of oil over 48 h of photo exposure. Furthermore, OV and CC demonstrate color change over time, while βCD-OV and βCD-CC remained constant. The results demonstrate that nanoencapsulation can be an interesting tool for protecting EOs.

Keywords Inclusion complexes · Thermal analysis; bioactivity

Supplementary Information The online version contains supplementary material available at https://doi.org/10.1186/s11671-024-04158-7.

✉ Fernanda Ramalho Procopio, nandaprocopio@gmail.com | [1]Brazilian Agricultural Research Corporation, Embrapa Instrumentation, São Carlos, SP 13561-206, Brazil. [2]Institute of Biosciences, Humanities and Exact Sciences, São Paulo State University (UNESP), São José Do Rio Preto, Brazil. [3]São Carlos Institute of Chemistry (IQSC), University of São Paulo (USP), São Carlos, São Paulo 13566-590, Brazil.

1 Introduction

The use of essential oils (EOs) as control agents in the agroindustry has been widely studied due to the varied composition of terpenes, aldehydes, alcohols, and phenols [1]. These compounds may have antioxidant, anti-inflammatory, antibacterial, antifungal, and insecticidal activity, arousing interest in the agricultural, food, and pharmaceutical industries. They appear as an alternative to synthetic additives, increasingly presenting undesirable side effects [2, 3].

Origanum vulgare (OV) and *Cymbopogon citratus* (CC) stand out in antifungal action due to their carvacrol/thymol and geranial/neral primary compounds, respectively [4]. Each oil's mechanisms and effectiveness are directly related to its chemical composition and, consequently, its stability. The compounds are susceptible to external factors such as temperature, oxygen, and light, and their bioactivity may be impaired [5]. Therefore, different strategies have been applied to improve stability and facilitate the incorporation of these extracts.

Combining nanotechnology strategies for incorporating essential oils can facilitate their application in foods, enhancing their properties. In general, micro or nanoencapsulation processes allow the packaging of bioactive compounds, seeking protection against external factors such as temperature, pH, oxygen, and interaction with other compounds [6]. The advantage of obtaining nanoscale particles is the increase in the surface area/volume ratio. In this way, more active sites are available, improving the encapsulated compound's bioavailability and consequently allowing greater interaction with enzymes and microorganisms [7].

Cyclodextrins (CD) are cyclic oligosaccharides composed of glucopyranose units linked by α-1,4 glycosidic bonds. The most common are α-cyclodextrin (six units), β-cyclodextrin (seven units), and γ-cyclodextrin (eight units). β-cyclodextrin (βCD) is the most used due to its ease of obtaining through synthesis, manufacturing, or extraction processes from natural sources [8]. The conical three-dimensional structure of CD molecules, with an internal cavity of lower polarity than water, is a key feature [6]. This structure allows for the retention of hydrophobic molecules such as essential oils in the internal cavity, leading to improved solubility in aqueous media. These properties make CDs suitable for a wide range of applications, including drug and pesticide delivery systems, flavor encapsulation, odor control, improving chemical stability and solubility, pollutant removal, and smart food packaging [9–11]. However, it is important to note that studying the most appropriate active and carrier ratio is necessary when forming essential oil inclusion complexes in CDs. Typically, an increase in this ratio can lead to a decrease in entrapment efficiency [12]. Nevertheless, CDs are considered nanoencapsulation agents, and the efficiency of the process is directly related to the stoichiometry and polarity of host and guest molecules [11].

Nanoencapsulated essential oils can promote a moderate release of compounds, prolonging antimicrobial activity with less sensorial impact on the food product [1, 13]. Ebrahimi et al.[14] observed a delay in ripening and microbial counts of pears when applying gluten-based coatings with cellulose nanoparticles containing oregano essential oil. Nevertheless, few studies have evaluated the efficiency of the encapsulation method on the stability of oils with different compositions.

In the study by Barbieri et al.[5], different *Lippia graveolens* chemotypes were encapsulated in β and γ-cyclodextrins (β-CD and γ-CD). The authors observed that oils rich in carvacrol and thymol showed the strongest affinity for γ-cyclodextrin, while those with β-caryophyllene presented higher encapsulation efficiency in β-cyclodextrin. In contrast, after 14 days of storage, carvacrol concentration in the β-CD complex remained constant, while in the γ-CD complex, the concentration was significantly reduced. The results indicate that interactions between the essential oil and the encapsulating material may influence stability.

In this context, this study aimed to investigate the effect of nanoscale β-cyclodextrin inclusion complexes on the thermal and photochemical stability of *Origanum vulgare* and *Cymbopogon citratus* essential oil. The complexes were characterized by morphology, size, entrapment efficiency, and thermal behavior. In addition, the compound's stability against exposure to UV light and temperature was evaluated in time intervals over 48 h.

2 Material and methods

2.1 Material

Oregano (*Origanum vulgare,* carvacrol 79.93%, thymol 5.00%, p-Cymene 4.81%) essential oil was purchased from Harmonie (Florianópolis, SC, Brazil) and Lemongrass (*Cymbopogon citratus,* neral 45.49%, geranial 36.19%, β-myrcene

5.48%) essential oil from Therra (Belo Horizonte, MG, Brazil). β-cyclodextrin used as coating material was purchased from (Sigma-Aldrich, Cotia-SP, Brazil). The reagents ethanol, ethyl acetate were of analytical grade.

2.2 Methods

2.2.1 Essential oils characterization

2.2.2 Nanoencapsulation via β-cyclodextrin inclusion complex

Nanoencapsulation of the *O. vulgare* (OV) and *C. citratus* (CC) essential oils was carried out through the formation of inclusion complexes in β-cyclodextrin (βCD), according to the methodology described by Wen et al.[15]. Different proportions (w/w) between encapsulating material (βCD) and essential oil were evaluated (100:0, 96:4, 92:8, 90:10, 88:12). Initially, β-cyclodextrin was dissolved in 90 ml of ethanol:water solution (1:2, v/v), kept under heating (55 ± 1 °C) and constant magnetic stirring for 3 h. After this period, OV and CC were dissolved in 10 ml of ethanol and slowly added to the βCD solution, dripping through a beaker. Heating and stirring were continued for another 2.5 h. Then, the mixture was cooled to room temperature and subsequently kept under refrigeration overnight for complete precipitation of the nanoparticles. The nanoencapsulated essential oils (βCD-OV and βCD-CC) were then recovered through centrifugation (9000 rpm, 4 °C, 10 min). The supernatant was discarded, and the precipitate was lyophilized. Finally, the dry powder was stored in sealed plastic bottles and kept in desiccators at room temperature until analysis was carried out.

2.2.3 Nanoparticles characterization

2.2.3.1 Process yield The yield of essential oil (EO) inclusion complexes was evaluated using equation (1):

$$Yield(\%) = \frac{mass\ of\ recovered\ powder(\beta CD - EO)(g)}{mass\ of\ \beta CD + mass\ of\ EO(g)} \times 100 \quad (1)$$

2.2.3.2 Entrapment efficiency The encapsulated essential oil content was determined according to the methodology described by Wen et al.[15], with modifications. The βCD-OV and βCD-CC (20-30 mg) complexes were washed with 10 ml of ethyl acetate for 30 seconds in a vortex to remove the surface oil. The liquid was discarded, and then 5 ml of distilled water and 5 ml of ethyl acetate were added to the washed powder to determine the inside oil content. The mixture was vortexed for 30 s and then kept in an ultrasonic bath at 40 °C for 5 min. An aliquot of 1 ml was then collected and added to 9 ml of ethyl acetate to read the absorbance on a UV-Vis spectrophotometer (UV-PC 1601, Shimadzu, Japan) at 275 nm (*O. vulgare*) and 254 (*C. citratus*). From the standard curves of OV ($Y=17.777x + 0.0062$; $R^2=0.9999$) and CC ($Y=27.073x + 0.0597$; $R^2=0.9931$), the entrapment efficiency (EE%) was determined using equation (2):

$$EE(\%) = \frac{EO\ content\ inside\ the\ particles}{EO\ concentration\ added} \times 100 \quad (2)$$

2.2.3.3 Size distribution—dynamic light scattering (DLS) The size distribution of *O. vulgare* and *C. citratus* inclusion complexes (βCD-OV and βCD-CC) was determined by the dynamic light scattering (DLS) technique using the Zetasizer Nano ZS equipment (Malvern Instruments, United Kingdom). Approximately 10-20 mg of each formulation was added to 10 ml of distilled water and placed in an ultrasonic bath at 25 °C for 3 min. Then, the samples were diluted in distilled water (1:10) to read (in triplicate) the size distribution and polydispersity index (PDI).

2.2.3.4 Morphology-scanning electron microscopy The morphology of the encapsulated essential oils (βCD-OV and βCD-CC) was evaluated through scanning electron microscopy (SEM) using a model microscope (JEOL-JSM 6510, Tokyo, Japan). The samples were deposited on double-sided carbon tape, fixed to the sample holder (stub), and coated with gold under vacuum. The images were captured with 5 kV voltage acceleration and x500 magnification.

2.2.3.5 Fourier transform infrared spectroscopy (FTIR) To evaluate chemical changes and possible interactions between essential oils, β-cyclodextrin and the inclusion complexes (βCD-OV and βCD-CC) were subjected to FTIR (Vertex 70, Bruker, Germany) in ATR mode. The spectra were recorded in the range of 4000 to 500 cm^{-1} with a resolution of 4 cm^{-1} in 32 scans.

2.2.3.6 Crystallinity The crystalline profile of the encapsulated oils (βCD-OV and βCD-CC) was analyzed using a DRX-6000 X-ray diffractometer (Shimadzu, Kyoto, Japan), with Cu-Kα radiation (λ = 1.5418 Å) in a 2θ range from 3° to 60° with steps of 0.02° at 1°/min.

2.2.3.7 Thermal behavior—differential scanning calorimetry (DSC) and thermogravimetry (TG/DTG) The thermal behavior of βCD, OV, CC, βCD-OV, and βCD-CC was evaluated by differential scanning calorimetry (DSC) using a DSC 60 Shimadzu (Japan). Approximately 5 mg of each sample was hermetically sealed in aluminum pans and subjected to a heating rate of 10 °C/min in the 20-200 °C temperature range under a dynamic nitrogen atmosphere (50 mL/min) [16]. The thermogravimetric curves (TG/DTG) were obtained on a DTG Shimadzu thermobalance (Japan) under a dynamic atmosphere of synthetic air (10 mL/min), a heating rate of 10 °C/min in the temperature range of 20-600 °C, using platinum pans with approximately 6 mg of samples.

2.2.3.8 Thermal and photo-stability The thermal and photo-sensibility of OV, CC, and inclusion complexes (βCD-OV and βCD-CC) were evaluated according to the methodology described by Qiao et al.[17], with slight modifications. Transparent 20 mL chromatography vials containing 0.02 g of each sample were sealed with a crimp cap and a perforated silicone septum. The vials were incubated in a drying oven without air circulation (Nova Ética, Brazil) at 70 °C for thermal stability. The photo-stability was evaluated by incubating the vials in a refrigerated photosensitization chamber (15 ° C) with 4 UV lamps (Philips 15 W G15T8). In both experiments, samples were evaluated in triplicate after 48 h, 24 h, 8 h, 4 h, 2 h, 1 h, and 30 min of exposure to heat or UV. After the exposure time, the free or encapsulated oil content was determined according to the previously described methodology (section 2.2.3.2).

2.2.3.9 Color variation after stress conditions Color changes of OV, CC, βCD-OV, and βCD-CC after 48h of thermal and photo stress period were evaluated using a Konica Minolta CR-400 colorimeter (Konica Minolta, Osaka, Japan) equipped with a C 2° illuminant using the CIELAB scale (L*: brightness, a*: (-) green to (+) red, and b*: (-) blue to (+) yellow)[18]. The total color difference (ΔE) was calculated with Equations (3), as follows:

$$\Delta E^* = \sqrt{\left[\left(L^*_{48} - L^*_0\right)^2 + \left(a^*_{48} - a^*_0\right)^2 + \left(b^*_{48} - b^*_0\right)^2\right]} \quad (3)$$

where L_0*, a_0* and b_0* correspond to the parameters evaluated at time zero and L_{48}*, a_{48}* and b_{48}* to the parameters evaluated after 48h of each stress exposure. According to Gonnet [19], the human eye can distinguish color variations for ΔE >1 values.

2.3 Statistical analysis

The data were statistically evaluated using the Minitab trial version program (Minitab 16.1.0, Minitab Inc., State College, PA, USA). The analysis of variance (ANOVA) and Tukey's test at a 5% probability level were applied.

3 Results and discussion

3.1 Process yield and entrapment efficiency

The formation of oregano essential oil inclusion complexes in β-cyclodextrin (βCD-OV) showed yields of 68-73%, while for lemongrass (βCD-CC), values between 68 and 83% were found (Table 1). Similar yield values were observed by Peng et al. [20] encapsulating star anise essential oil in β-cyclodextrin complexes. These variations may be related

Table 1 Inclusion complexes process parameters

Formulation	Yield (%)	Entrapment efficiency (%)	Mean particle size (nm)	PDI
βCD	56.3 ± 8.1^{e}	–	770.1 ± 85.6^{b}	0.64 ± 0.0^{abc}
βCD-OV(96:4)	72.0 ± 6.3^{cd}	30.1 ± 13.1^{c}	1047.2 ± 139.3^{a}	0.62 ± 0.1^{bc}
βCD-OV(92:8)	68.4 ± 2.7^{d}	73.0 ± 5.6^{a}	541.7 ± 33.4^{cd}	0.60 ± 0.0^{bc}
βCD-OV(90:10)	72.9 ± 0.2^{bcd}	72.5 ± 11.7^{a}	338.3 ± 47.8^{de}	0.97 ± 0.0^{a}
βCD-OV(88:12)	72.3 ± 0.9^{bcd}	58.0 ± 7.4^{ab}	267.8 ± 29.2^{e}	0.46 ± 0.0^{c}
βCD-CC(96:4)	68.6 ± 1.4^{d}	45.9 ± 4.8^{bc}	518.6 ± 77.1^{c}	0.78 ± 0.2^{ab}
βCD-CC(92:8)	80.0 ± 2.1^{abc}	54.7 ± 8.0^{abc}	413.1 ± 102.5^{cd}	0.55 ± 0.1^{c}
βCD-CC(90:10)	83.4 ± 0.5^{a}	57.0 ± 9.0^{ab}	443.3 ± 68.5^{cd}	0.52 ± 0.2^{c}
βCD-CC(88:12)	81.6 ± 1.7^{ab}	48.6 ± 4.2^{bc}	418.9 ± 120.5^{cd}	0.64 ± 0.1^{bc}

*PDI: polydispersity index

*Different lowercase letters in the same column indicate a significant statistical difference using the Tukey test ($p \leq 0.5$)

to the difference in polarity between essential oils, which influences their affinity with the βCD hydrophobic cavity. According to Marques et al. [11], due to the varied composition of essential oils, the most hydrophobic components will be preferentially incorporated into the β-cyclodextrin cavity. In this case, some of the compounds may not be complexed, reducing yield.

The entrapment efficiency was influenced by the ratio between encapsulating material (βCD) and essential oil, being higher for ratios of 92:8 and 90:10 (Table 1). In the study by Kong et al.[21], the 1:9 ratio between tea tree oil (*Melaleuca alternifolia*) and βCD also resulted in greater entrapment efficiency. Typically, in pharmaceutical applications, isolated compounds are encapsulated in βCD with an optimal stoichiometric ratio of 1:1 [22]. For essential oils (EOs), this proportion may not be met. Ayala-Zavala et al.[23] suggest that the interior cavity of βCD has a limited capacity for trapping compounds of varying chemical nature. In this sense, an increase in essential oil concentration can decrease entrapment efficiency, as evidenced in Table 1 for the ratio of 88:12 (βCD-OV and βCD-CC).

3.2 Particle size distribution and morphology

Differences on size (Table 1) and morphology (Figure 1) of empty nanoparticles (βCD) and those containing essential oils (βCD-OV and βCD-CC) were observed. For the control formulation (Figure 1), irregular-shaped structures between 200-900 nm were observed, presenting cracks on the surface and mean particle size of 770.1 ± 85.6 (Table 1). Samples containing *O. vulgare* essential oil (Figure 1) showed trapezoidal-shaped particles, smaller sizes (except for βCD-OV 96:4), and a tendency to aggregate. These aggregates can interfere with light scattering during particle size reading [24]. Indeed, even with smaller particles appearing in the micrographs (Figure 1), the size distribution of some oil-containing formulations (βCD-OV 96:4, βCD-OV 92:8) covers a broader range between 100 and 1000 nm. Formulations βCD-OV 96:4 and βCD-OV 92:8 presented the highest mean particle size (1047.2 ± 139.3 and 541.7 ± 33.4, respectively) values which was confirmed by the presence of larger particles on micrographs. Furthermore, regions of particle clusters of smaller sizes were observed (Figure 1) for formulations containing higher essential oil concentrations (βCD-OV 90:10 and βCD-OV 88:12). These small structures grouped can also explain the high PDI values. Similar results were observed by Hosseini et al.[25] by encapsulating oregano essential oil in chitosan nanoparticles. The author observed an increase in particle size for higher essential oils content, reaching average particle sizes of 400 nm. This result may be related to the surface oil content, explained by the reduction in entrapment efficiency (Table 1).

For the inclusion complexes containing *C. citratus* (Figure 2), flat plate structures with cracks and sizes between 300-800 nm were observed for the βCD-CC 96:4 and βCD-CC 92:8 formulations. The βCD-CC 90:10 and βCD-CC 88:12 formulations presented trapezoidal morphology, mean particle size of 443.3 ± 68.5 and 418.9 ± 120.5, respectively, and a smooth surface, indicating greater entrapment efficiency. Anaya-Castro et al.[26] explain that small fissures and striations on the surface of β-cyclodextrin inclusion complexes favor the expulsion of volatiles, reducing entrapment efficiency.

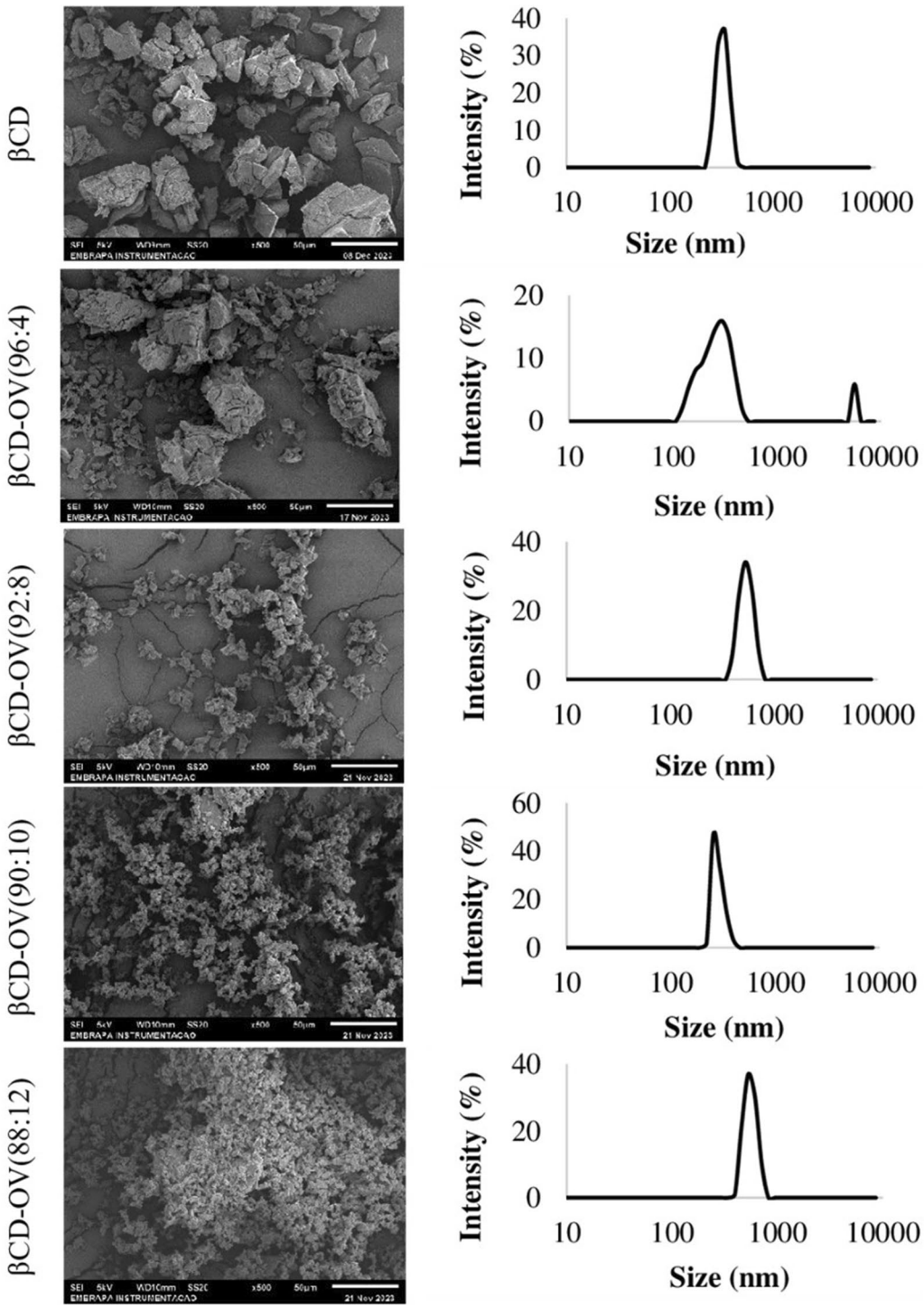

Fig. 1 Micrographs and size distribution of pure β-cyclodextrin (βCD) and inclusion complexes with *O. vulgare* essential oSil (βCD-OV) in different proportions

3.3 Fourier transform infrared spectroscopy (FTIR)

Figure 3a shows the FTIR spectra of β-cyclodextrin (βCD), *O. vulgare* (OV) and their inclusion complexes (βCD-OV). The spectra of pure and encapsulated C. *citratus* (CC and βCD-CC, respectively) are shown in Figure 3b. In the βCD spectrum (Figure 3a), characteristic bands at 3290 cm^{-1} and 1028 cm^{-1} correspond to the stretching of the O-H and

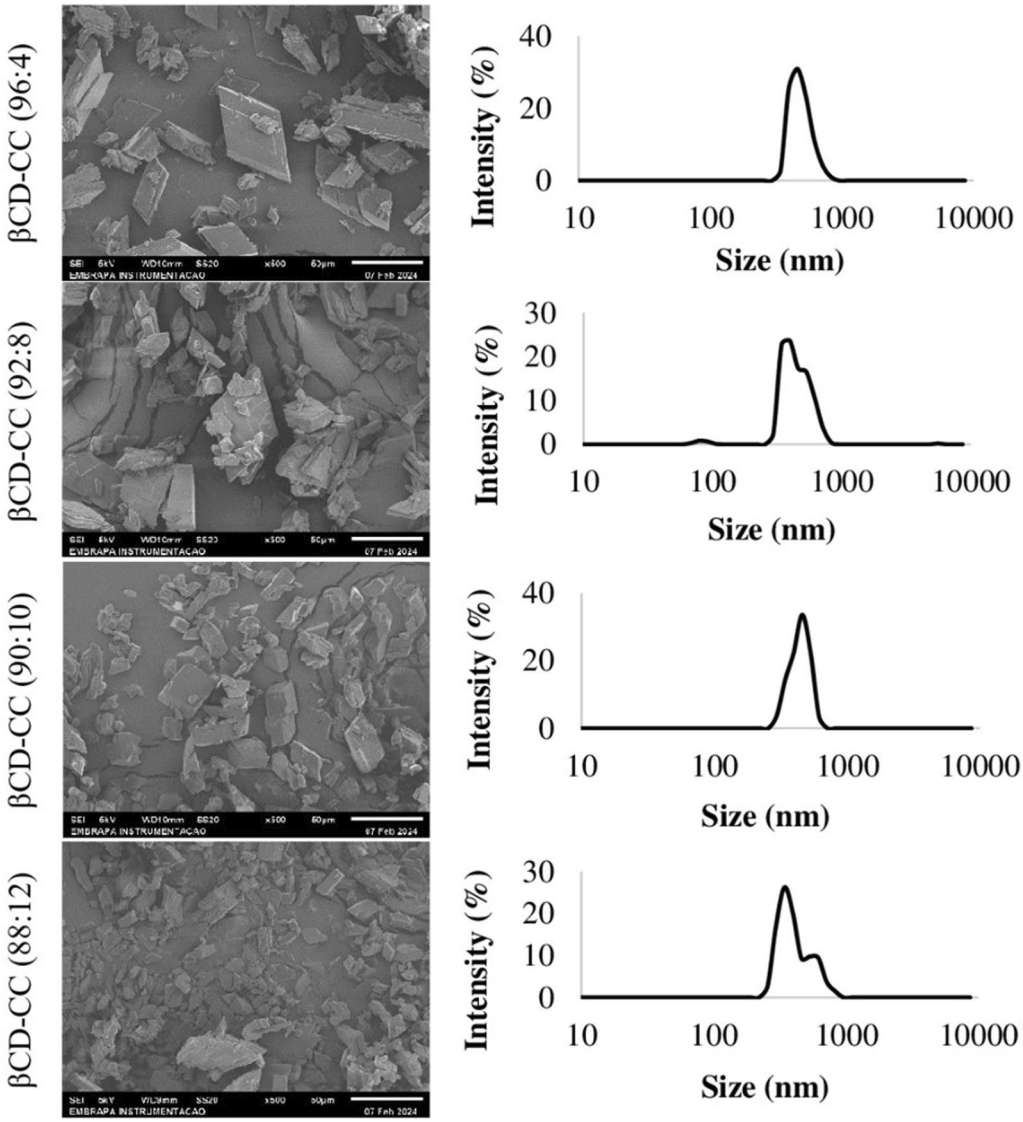

Fig. 2 Micrographs and size distribution of β-cyclodextrin (βCD) inclusion complexes with *C. citratus* essential oil (βCD-OV) in different proportions

C-O-C groups, respectively [16]. For *O. vulgare* oil, peaks between 800 and 1500 cm^{-1} are attributed to the presence of carvacrol, its primary compound, while the peak close to 2955 cm^{-1} is related to the C-H stretching of aromatic rings, common in essential oils [27, 28]. For *C. citratus* oil (Figure 3b), characteristic peaks at 2910 cm^{-1} and 1674 cm^{-1} are related to the stretching of the C-H bond and vibrations of the C=O bonds present in citral, respectively [29]. Analyzing the inclusion complexes spectra of *O. vulgare* (βCD-OV) and *C. citratus* (βCD-CC), the suppression of the characteristic peaks of the free oils (2955 and 1674 cm^{-1}, respectively) indicates the compounds immobilization through nanoencapsulation. The oil accommodation inside the βCD cavity restricts the vibration of reactive groups, indicating the formation of the complex. Silva et al.[30] observed similar behavior by forming inclusion complexes between 6-gingerol and βCD.

3.4 Crystallinity

The crystalline pattern of the inclusion complexes with *O. vulgare* (Fig. 4a) and *C. citratus* (Fig. 4b) differed from the pure βCD. Characteristics peaks at 5°, 9.4°, 12.8°, 22.9°, 27.2°, 32.3°, 35° and 40.9 were observed for βCD, as reported by Jiang et al.[16]. This XRD pattern corresponds to the "cage" crystalline structure. In the "cage" form, the βCD cavity is

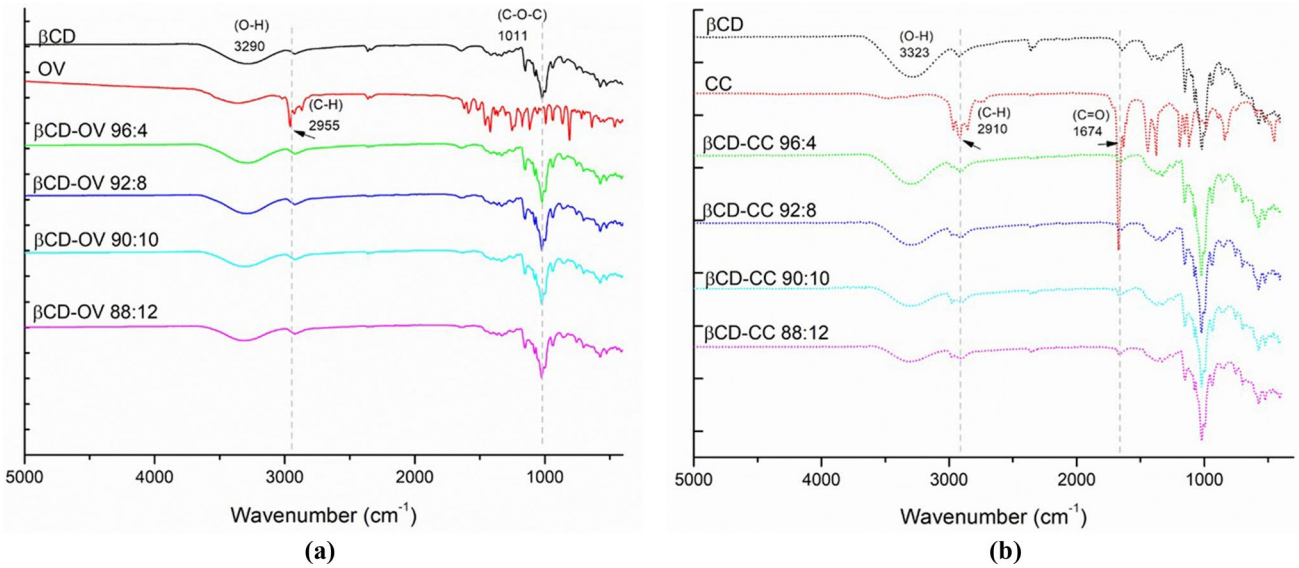

Fig. 3 FTIR spectra of the inclusion complexes of **a** Origanum vulgare (βCD-OV*)* and**b** Cymbopogon citratus (βCD-CC) with β-cyclodextrin (βCD)

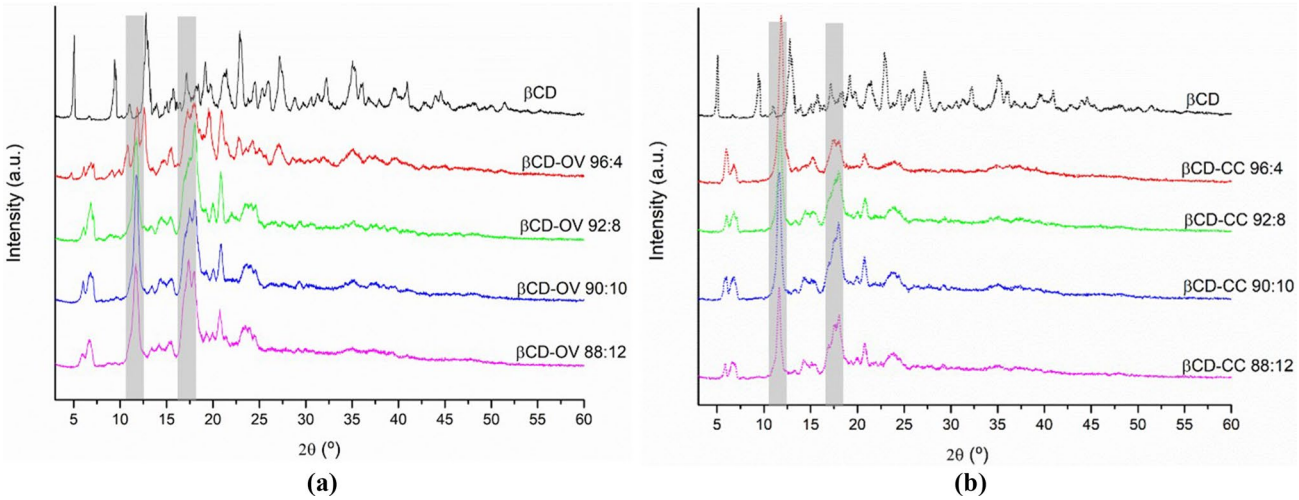

Fig. 4 Diffractograms of the inclusion complexes of **a Origanum vulgare** (βCD-OV*)* and **bCymbopogon citratus** (βCD-CC) with β-cyclodextrin (βCD)

blocked by neighboring molecules, making it unavailable to form a micro/nanocapsule with central molecules [21]. The disappearance of the peak at 9.6° and the appearance of a sharp peak at 11.8° followed by a broadened peak between 18° and 19° (highlighted in grey) in the complexes diffractograms (βCD-OV and βCD-OV) suggests a change in the crystalline conformation, confirming the complexation. Jiang et al.[16] also observed this behavior in the formation of catechin/β-cyclodextrin complexes. During the formation of inclusion complexes, the "cage" structure is converted into a "channel-type", where the βCD molecules stack on each other, forming long cylindrical channels [21], resulting in a different crystalline pattern.

3.5 Thermal behavior

Figure 5a-b shows the thermal curves of βCD, OV, CC, βCD:OV, and βCD:CC complexes. For βCD, a single endothermic peak is observed at 115 ºC, related to residual humidity. Regarding the essential oils, *O. vulgare* (Fig. 5a) showed successive melting events in the 95 to 124 ºC range, and *C. citratus* (Fig. 5b) presented two sharp endothermic peaks at 158 ºC

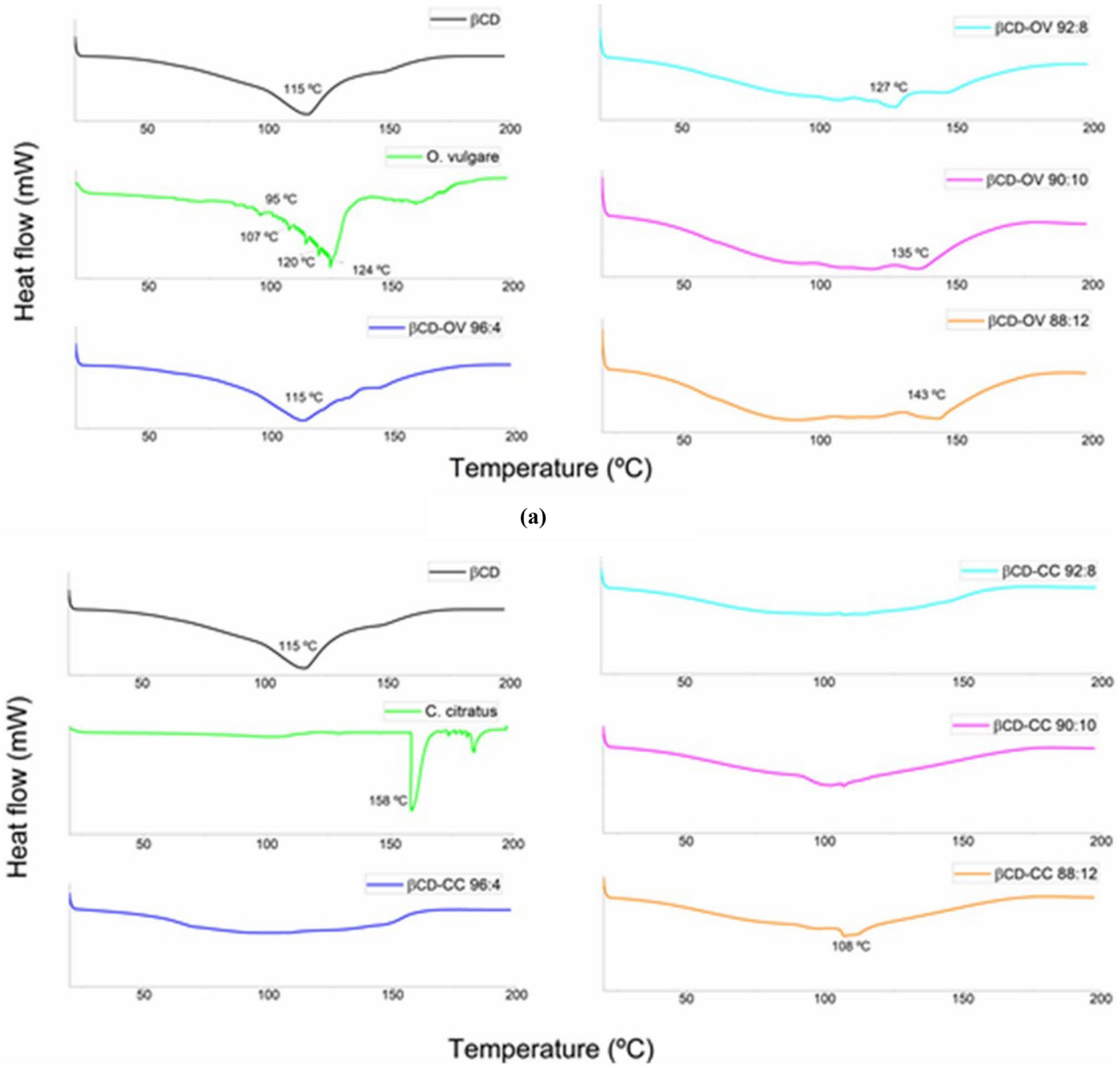

Fig. 5 DSC curves of the inclusion complexes of **a** *Origanum vulgare* (βCD-OV) and **b** *Cymbopogon citratus* (βCD-CC) with β-cyclodextrin (βCD)

and 183 °C. Compounds of different chemical natures explain this behavior. Except for the βCD:OV (96:4) formulation, which showed similar behavior to pure βCD, the endothermic events of the encapsulated *O. vulgare* samples (βCD-OV 92:8, βCD-OV 90:10, βCD-OV 88:12) appear displaced (Fig. 5a), reaching a wider temperature range (88–150 °C). This result indicates that the inclusion of *O. vulgare* in β-cyclodextrin delays the compounds volatilization, providing greater thermal stability.

For the *C. citratus* complexes (βCD-OV 92:8, βCD-OV 90:10, βCD-OV 88:12 (Fig. 5b), the pronounced peaks at 158 °C and 183 °C observed for the pure oil disappeared, indicating immobilization of the compounds. Rodrigues et al.[31] observed a similar result by encapsulating *Ocimum basilicum* essential oil in β-cyclodextrin. The authors suggest that the absence of endothermic events in the encapsulated oil curve indicates a greater affinity between the volatile compounds and the hydrophobic cavity of βCD.

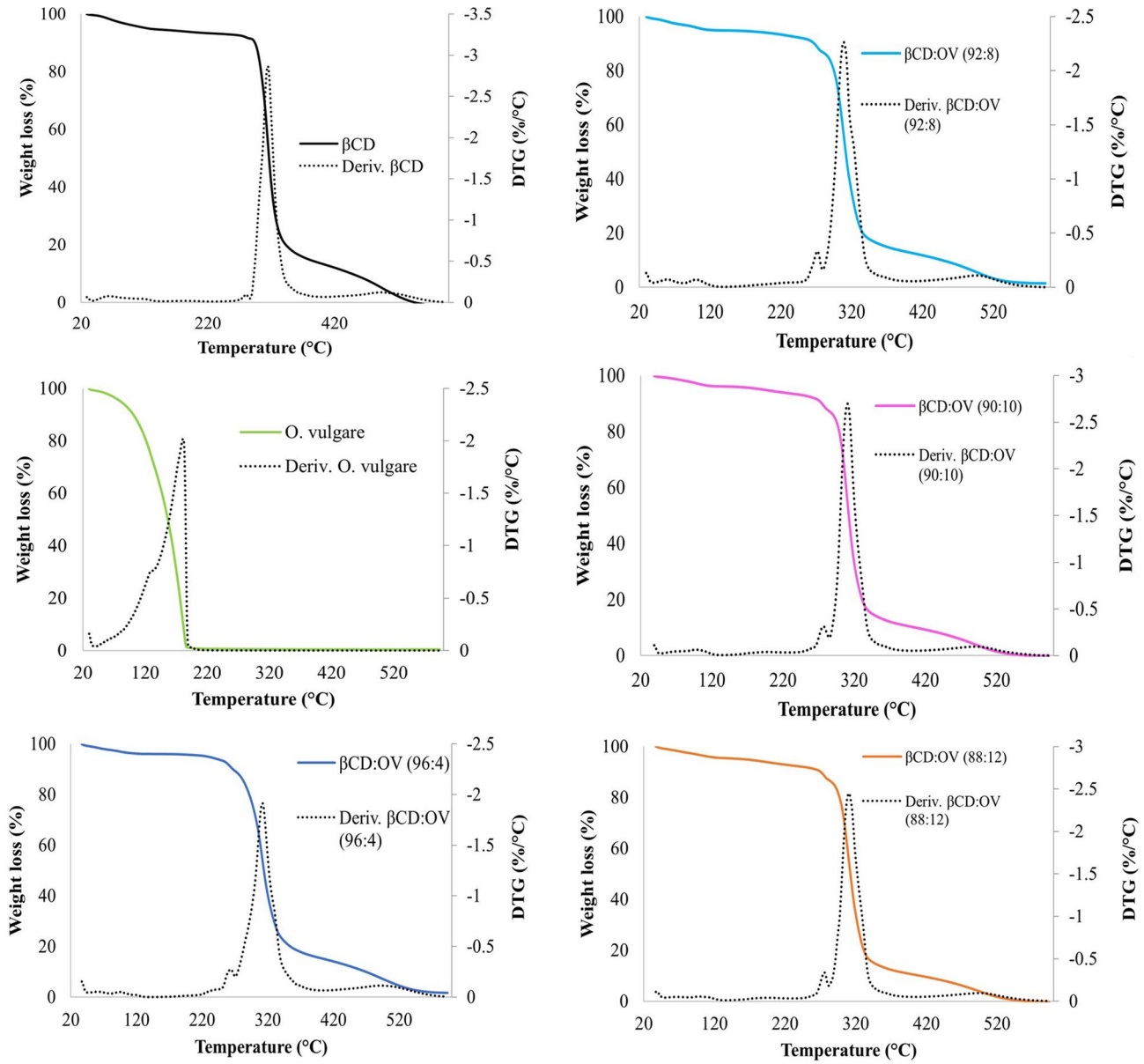

Fig. 6 TG and DTG curves of the inclusion complexes of *Origanum vulgare* (βCD-OV*)* with β-cyclodextrin (βCD)

Thermogravimetric curves (TG) and derivative TG (DTG) of *O. vulgare* (OV), *C. citratus* (CC) β-ciclodextrin (βCD) and their inclusion complexes (βCD-OV and βCD-CC) are show in Figs. 6–7. For βCD (Fig. 6), two events are observed. The first (70–120 ºC) represents a 6% mass reduction related to dehydration [31]. The second appears between 300 and 335 °C, representing a mass loss of 75%, indicating the temperature range where the βCD undergoes degradation. For free OV (Fig. 6), it is observed that the mass loss occurs in a single event between 20 and 220 °C. As for the βCD-OV encapsulated oil curves (Fig. 6), the appearance of a lower intensity peak between 220 and 270 °C indicates the formation of complexes capable of delaying the volatilization of the compounds. Similar behavior was observed by Marques et al.[32] by encapsulating basil essential oil (*Pimenta dioica*) in β-cyclodextrin. The authors suggest that the complexation between oil and βCD was evidenced by the appearance of a second stage of degradation at higher temperatures than the pure oil. Figure 6 also shows slight inflections in the region between 60 and 220 °C for the βCD-OV 92:8, βCD-OV 90:10, and βCD-OV 88:12 formulations. Such behavior may be related to degradation events triggered by the interaction between βCD and OV. The stability results discussed in the next section support this hypothesis.

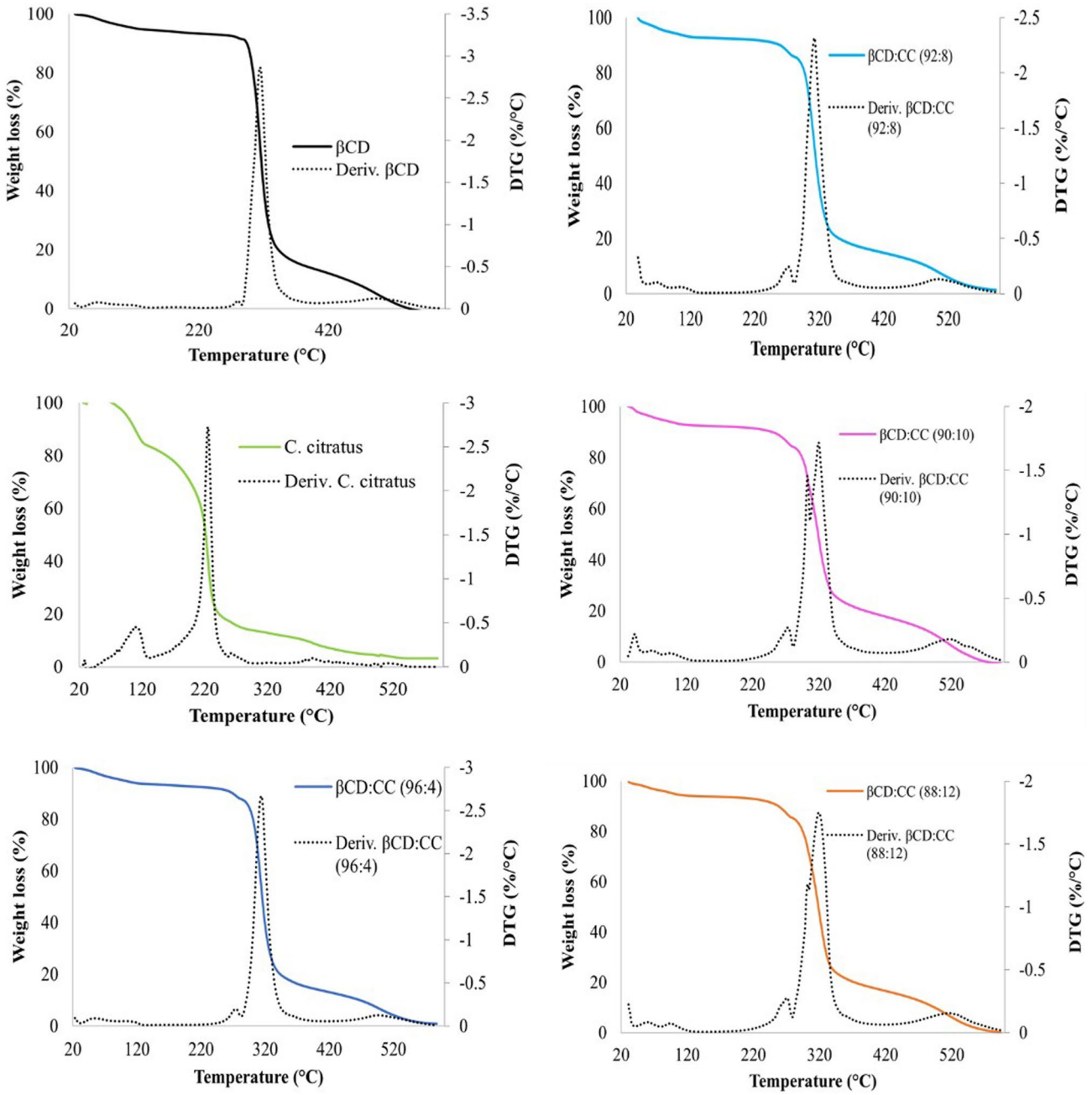

Fig. 7 TG and DTG curves of the inclusion complexes of *Cymbopogon citratus* (βCD-CC*)* with β-cyclodextrin (βCD)

The thermogravimetric curve of *C. citratus* (Fig. 7) shows that degradation occurs in two main stages. The first between 20–120 °C corresponds to a mass loss of 20%, while 60% is lost between 170–270 °C. Less significant fractions appear close to 400 °C. Regarding βCD-CC 96:4, βCD-CC 92:8, βCD-CC 90:10, and βCD-CC 88:12 curves (Fig. 7), the disappearance of the first degradation peak (20–120 °C) evidences the protective effect of inclusion complexes. Moreover, a slight peak appears close to 260 °C, suggesting that volatilization was delayed. As observed for *O. vulgare* complexes, minimal inflections appear below 220 °C, which may be related to βCD-CC interactions. In the study by Martins et al.[29], a single peak of *C. citratus* degradation between 106–150 °C was observed, corresponding to a mass loss of almost 90%. Similarly, the authors observed the effect of encapsulation through the appearance of a lower intensity peak between 180-220°C for formulations containing *C. citratus,* maltodextrin, and gelatin.

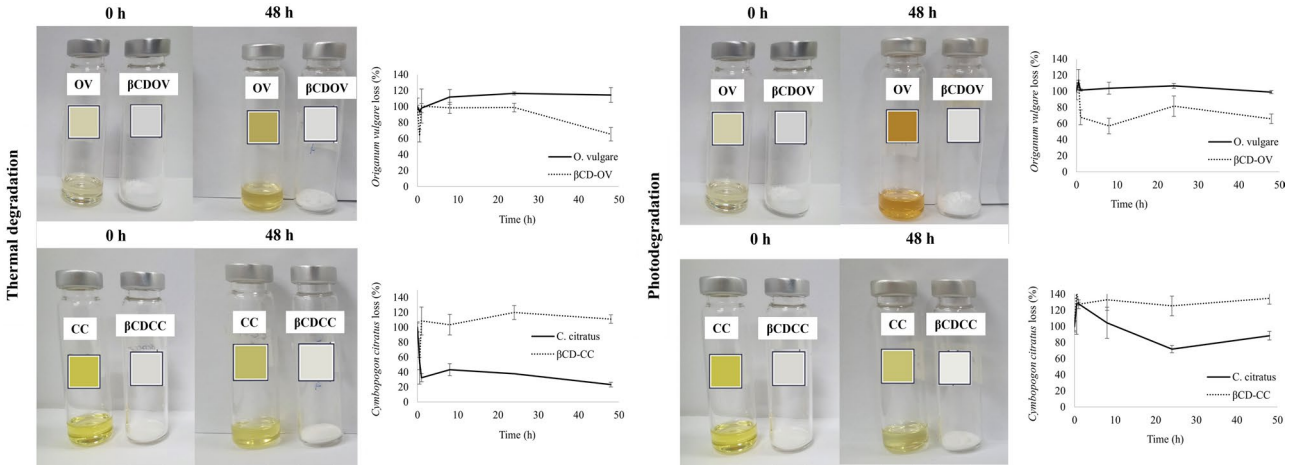

Fig. 8 Thermal (**a**) and photo-stability (**b**) of *Origanum vulgare* (OV), *Cymbopogon citratus* (CC) and their inclusion complexes with β-cyclodextrin (βCD)

3.6 Color variation, thermal and photo-stability

Formulations with a 90:10 ratio between βCD and essential oils (OV and CC) were selected for the stability study because they present greater entrapment efficiency and more homogeneous morphology and size distribution. The thermal and photodegradation spectrophotometric curves of free and encapsulated *O. vulgare* and *C. citratus* are shown in Fig. 8a-b.

Exposure to heat led to changes in the color of free essential oils (Fig. 8a). OV turned from pale yellow to light orange, reaching an ΔE of 13.1 ± 2.1 (Table 2, supplementary material), while CC demonstrated less color variation (ΔE = 5.3 ± 1.4), going from bright yellow to light yellow. Nevertheless, exposure to UV light suggests a more significant degradation of OV and CC oils. The OV went from pale yellow to dark orange (ΔE = 13.6 ± 1.1), while the CC went from bright yellow to pale yellow (ΔE = 11.6 ± 3.6). Park et al.[18] also observed a greater effect of light on the color change of fresh kunzea (*Kunzea ambigua)* essential oil after eight months of storage.

Despite the color change, no significant differences were observed in the OV absorption spectrum, reflecting minimal variations in the release curve after thermal (Fig. 8a) and photodegradation (Fig. 8b). For CC, thermal stress caused a 50% loss in oil content after 30 min of exposure (Fig. 8a). In photodegradation (Fig. 8b), this reduction was observed after 24 h of conditioning.

Degradation compounds can be generated over time due to stressful conditions [33]. If the absorption spectrum is the same as the primary compounds, the absorbance may be balanced, and the reading may be masked. This may explain the constancy in the OV spectrophotometric curve. Indeed, Odak et al.[34] observed a decrease of *trans*-caryophyllene with a simultaneous increase of caryophyllene oxide, a well-known secondary oxidation product, evaluating the stability of *Satureja montana* and *Lavandula angustifolia* essential oils against light and temperature. The authors observed a color change in *S. montana* oil triggered by irradiation, going from pale yellow to orange. They point out that polymerization reactions can be responsible. Najafian [33] observed a similar result when evaluating the aging of *Melissa officinalis* L. essential oil under refrigeration and freezing conditions. The authors observed a significant decay of geranial and neral compounds over the four months of storage. UV-radiation also causes cyclization of citral, the majority of Lemongrass essential oil, promoting significant flavor changes, as pointed out by Marques et al. [11].

Encapsulation processes aim to improve volatile compounds' stability, protecting them against external factors[6]. Indeed, no color change was observed for βCD:OV and βCD:CC complexes. Regarding the spectrophotometric curve, the encapsulated OV content remains constant for up to 24 h of thermal stress (Fig. 8a), with a 40% reduction after 48 h of exposure. In photodegradation, this loss is reached after one hour of exposure (Fig. 8b), with slight variations until the end of the stress period. These results may be related to interactions between βCD and OV stimulated by stress agents. As observed in the thermogravimetric curves (Fig. 6), decomposition reactions of the βCD:OV complexes appear in the temperature range of the study (70 °C). In this case, polymerization reactions may have occurred [34], resulting in changes in the molecular organization and the release of the trapped oil. For the βCD-CC complexes, the oil content remained constant throughout the thermal and photo stress period, demonstrating good protection for the compounds.

These findings highlight the potential of β-cyclodextrin inclusion complexes in protecting essential oils. This characteristic positions them as strong candidates for use in various areas, such as pharmaceuticals, cosmetics, perfumery, environmental, agriculture and the food industry [9]. Given this versatility, a promising application is in post-harvest technology, where they can be used as additive for synthesizing edible films and coatings [10]. These complexes can then be applied as controlled release systems of essential oil in fruit coatings, potentially reducing spoilage of fruits and vegetables without compromising their sensory qualities. Future research focused on the effects of incorporating β-cyclodextrin into coatings could lead to significant advances in agricultural and food sciences.

4 Conclusion

The study demonstrated that the nanoencapsulation of *O. vulgare (OV)* and *C. citratus (CC)* essential oil (EO) in β-cyclodextrin (βCD) resulted in crystalline structures of varied sizes (200 to 800 nm), trapezoidal shape and tendency to aggregation. The highest entrapment efficiency was obtained in βCD-EO proportions of 92:8 and 90:10. Characterization by XRD, FTIR, DSC, and TGA confirmed the oil entrapment and the formation of inclusion complexes. Converting a liquid material into nanosized crystalline structures facilitates essential oil handling and application. Furthermore, the nanometric complexes prevented color changes in OV and free CC caused by thermal and photo stability. The βCD-OV complexes also prevented compound loss during 24 h of thermal stress and 48 h of UV exposure. For βCD-CC, the compounds remained constant during the 48 h of both stress periods. Further investigation regarding changes in the chemical composition of degraded EOs should be conducted. The results demonstrate that combining nanotechnology strategies can maintain the integrity of essential oils during stress conditions. These findings are interesting for further studies applying encapsulated essential oils as antimicrobial agents.

Author contribution Author Contributions Statement F.R.P: Conceptualization, Investigation, Methodology, Formal analysis, Data curation, Visualization, Writing–original draft; R.P.B: Methodology, Investigation, Validation, Writing – review; L.E.S.V: Investigation, Data curation, Validation, Writing – review; M.E.M.M: Investigation, Data curation, Validation, Writing – review; M.E.A.A: Investigation, Data curation, Validation; S.B.J: Validation, Writing – review; M.D.F: Conceptualization, Supervision, Methodology, Validation, Writing – review & editing, Resources, Project administration, Funding acquisition.

Funding This research was supported by the FAPESP grants (process 2022/10686–6, 2022/03229–8, fellowships 2023/14371–2, 2023/17653–9), Empresa Brasileira de Pesquisa Agropecuária – Embrapa, Rede Agronano, and CNPq/MCTI Sisnano (process 442575/2019–0, fellowships #383538/2023–8, #385552/2023–8, #138584/2023–0) and M.D.Ferreira CNPq Research Productivity fellowship (#307141/2022–5). The authors also acknowledge the support from "Coordenação de Aperfeiçoamento de Pessoal de Nível Superior" (CAPES-Brazil; Finance code 001). The opinions, hypotheses, and conclusions or recommendations expressed in this article are the responsibility of the author(s) and do not necessarily reflect the view of FAPESP.

Data Availability The authors declare that the data supporting the findings of this study are available within the paper and its supplementary information files.

Declarations

Competing interests The authors declare no competing interests.

References

1. de Carvalho APA, Conte-Junior CA. Nanoencapsulation application to prolong postharvest shelf life. Curr Opin Biotechnol. 2022;78:102825. https://doi.org/10.1016/j.copbio.2022.102825.

2. Ghosoph JM, Schmidt LS, Margosan DA, Smilanick JL. Imazalil resistance linked to a unique insertion sequence in the PdCYP51 promoter region of Penicillium digitatum. Postharvest Biol Technol. 2007;44:9–18. https://doi.org/10.1016/j.postharvbio.2006.11.008.
3. Leite ICHL, Silva RA, Santos JECC, Freitas-Lopes RL, Câmara MPS, Michereff SJ, Lopes UP. Analysis of *Colletotrichum musae* populations from Brazil reveals the presence of isolates with high competitive ability and reduced sensitivity to postharvest fungicides. Plant Pathol. 2020;69:1529–39. https://doi.org/10.1111/ppa.13229.
4. da Costa GD, Ribeiro WR, Gonçalves DC, Menini L, Costa H. Recent advances and future perspective of essential oils in control Colletotrichum spp.: A sustainable alternative in postharvest treatment of fruits. Food Res Int. 2021;150:110758.
5. Barbieri N, Sanchez-Contreras A, Canto A, Cauich-Rodriguez JV, Vargas-Coronado R, Calvo-Irabien LM. Effect of cyclodextrins and Mexican oregano (Lippia graveolens Kunth) chemotypes on the microencapsulation of essential oil. Ind Crops Prod. 2018;121:114–23. https://doi.org/10.1016/j.indcrop.2018.04.081.
6. Assadpour E, Jafari SM. Nanoencapsulation. In: Nanomaterials for Food Applications. Elsevier; 2019. p. 35–61. https://doi.org/10.1016/B978-0-12-814130-4.00003-8.
7. McClements DJ. Nanoscale nutrient delivery systems for food applications: improving bioactive dispersibility stability, and bioavailability. J Food Sci. 2015. https://doi.org/10.1111/1750-3841.12919.
8. Song Q, Lu Q, Zhang S, Zhang Z, Huang J, Li X, Song D, Pu J, Yang Z, Fang Z, Liu Y, Hu B. Preparation and characterization of fennel (Foeniculum vulgare miller) essential oil/hydroxypropyl-β-cyclodextrin inclusion complex and its application for chilled pork preservation. Food Chem. 2024;456:139887. https://doi.org/10.1016/j.foodchem.2024.139887.
9. Del Valle EMM. Cyclodextrins and their uses: a review. Process Biochem. 2004;39:1033–46. https://doi.org/10.1016/S0032-9592(03)00258-9.
10. Liu Y, Sameen DE, Ahmed S, Wang Y, Lu R, Dai J, Li S, Qin W. Recent advances in cyclodextrin-based films for food packaging. Food Chem. 2022;370:131026. https://doi.org/10.1016/j.foodchem.2021.131026.
11. Marques HMC. A review on cyclodextrin encapsulation of essential oils and volatiles. Flavour Fragr J. 2010;25:313–26. https://doi.org/10.1002/ffj.2019.
12. Fenyvesi E, Szente L. Nanoencapsulation of flavors and aromas by cyclodextrins. In: Encapsulations. Elsevier; 2016. p. 769–92. https://doi.org/10.1016/B978-0-12-804307-3.00018-1.
13. Donsì F, Annunziata M, Sessa M, Ferrari G. Nanoencapsulation of essential oils to enhance their antimicrobial activity in foods. LWT Food Sci Technol. 2011;44:1908–14. https://doi.org/10.1016/j.lwt.2011.03.003.
14. Ebrahimi R, Fathi M, Ghoddusi HB. Nanoencapsulation of oregano essential oil using cellulose nanocrystals extracted from hazelnut shell to enhance shelf life of fruits: Case study: Pears. Int J Biol Macromol. 2023;242:124704. https://doi.org/10.1016/j.ijbiomac.2023.124704.
15. Wen P, Zhu D-H, Feng K, Liu F-J, Lou W-Y, Li N, Zong M-H, Wu H. Fabrication of electrospun polylactic acid nanofilm incorporating cinnamon essential oil/ β -cyclodextrin inclusion complex for antimicrobial packaging. Food Chem. 2016;196:996–1004. https://doi.org/10.1016/j.foodchem.2015.10.043.
16. Jiang L, Yang J, Wang Q, Ren L, Zhou J. Physicochemical properties of catechin/β-cyclodextrin inclusion complex obtained via co-precipitation. CyTA—J Food. 2019;17:544–51. https://doi.org/10.1080/19476337.2019.1612948.
17. Qiao X, Jiang Y, Duan R, Li Z, Kong Z, Zhang L, Dai L, Wang Y, Sun Q, McClements DJ, Wang C, Xu X. Fabrication of curcumin-loaded pea protein isolate-quillaja saponin-tannic acid self-assembled nanoparticles by tuning non-covalent interactions: Enhanced physicochemical, interfacial and emulsifying properties. Food Hydrocoll. 2024;148:109436. https://doi.org/10.1016/j.foodhyd.2023.109436.
18. Park C, Garland SM, Close DC. The influence of temperature, light, and storage period on the colour and chemical profile of kunzea essential oil (Kunzea ambigua (Sm.) Druce). J Appl Res Med Aromatic Plants. 2022;30:100383. https://doi.org/10.1016/j.jarmap.2022.100383.
19. Gonnet J-F. Colour effects of co-pigmentation of anthocyanins revisited—1. A Colorimet Defin Using CIELAB Scale Food Chem. 1998;63:409–15. https://doi.org/10.1016/S0308-8146(98)00053-3.
20. Peng Q, Luo X, Su J, Bi Y, Kong F, Wang Z, Tan S, Zhang J. Microencapsulation of star anise essential oil: Preparation, characterization, in vitro digestion, and biological activity. Colloids Surf A Physicochem Eng Asp. 2024;696:134358. https://doi.org/10.1016/j.colsurfa.2024.134358.
21. Kong P, Abe JP, Masuo S, Enomae T. Preparation and characterization of tea tree oil-β-cyclodextrin microcapsules with super-high encapsulation efficiency. J Bioresour Bioprod. 2023;8:224–34. https://doi.org/10.1016/j.jobab.2023.03.004.
22. Wang H, Luo J, Zhang Y, He D, Jiang R, Xie X, Yang Q, Li K, Xie J, Zhang J. Phospholipid/hydroxypropyl-β-cyclodextrin supramolecular complexes are promising candidates for efficient oral delivery of curcuminoids. Int J Pharm. 2020;582:119301. https://doi.org/10.1016/j.ijpharm.2020.119301.
23. Ayala-Zavala JF, Soto-Valdez H, González-León A, Álvarez-Parrilla E, Martín-Belloso O, González-Aguilar GA. Microencapsulation of cinnamon leaf (Cinnamomum zeylanicum) and garlic (Allium sativum) oils in β-cyclodextrin. J Incl Phenom Macrocycl Chem. 2008;60:359–68. https://doi.org/10.1007/s10847-007-9385-1.
24. Raval N, Maheshwari R, Kalyane D, Youngren-Ortiz SR, Chougule MB, Tekade RK. Importance of physicochemical characterization of nanoparticles in pharmaceutical product development. In: Basic Fundamentals of Drug Delivery. Elsevier; 2019. p. 369–400. https://doi.org/10.1016/B978-0-12-817909-3.00010-8.
25. Hosseini SF, Zandi M, Rezaei M, Farahmandghavi F. Two-step method for encapsulation of oregano essential oil in chitosan nanoparticles: preparation, characterization and in vitro release study. Carbohydr Polym. 2013;95:50–6. https://doi.org/10.1016/j.carbpol.2013.02.031.
26. Anaya-Castro MA, Ayala-Zavala JF, Muñoz-Castellanos L, Hernández-Ochoa L, Peydecastaing J, Durrieu V. β-Cyclodextrin inclusion complexes containing clove (Eugenia caryophyllata) and Mexican oregano (Lippia berlandieri) essential oils: preparation, physicochemical and antimicrobial characterization, food packag shelf. Life. 2017;14:96–101. https://doi.org/10.1016/j.fpsl.2017.09.002.
27. Hernández-Nava R, López-Malo A, Palou E, Ramírez-Corona N, Jiménez-Munguía MT. Encapsulation of oregano essential oil (Origanum vulgare) by complex coacervation between gelatin and chia mucilage and its properties after spray drying. Food Hydrocoll. 2020;109:106077. https://doi.org/10.1016/j.foodhyd.2020.106077.
28. Valderrama AC, De GC. Traceability of active compounds of essential oils in antimicrobial food packaging using a Chemometric method by ATR-FTIR. Am J Anal Chem. 2017;8(11):726–41.

29. da Silva MW, de Araújo JS, Feitosa BF, Oliveira JR, Kotzebue LR, da Silva Agostini DL, de Oliveira DL, Mazzetto SE, Cavalcanti MT, da Silva AL. Lemongrass (cymbopogon citratus DC. Stapf) essential oil microparticles: development, characterization, and antioxidant potential. Food Chem. 2021;355:129644.
30. da Silva JA, Sampaio PA, Dulcey LJL, Cominetti MR, Rabello MM, Rolim LA. Preparation and characterization of [6]-gingerol/β-cyclodextrin inclusion complexes. J Drug Deliv Sci Technol. 2021;61:102103. https://doi.org/10.1016/j.jddst.2020.102103.
31. L.B. Rodrigues, A.O.B.P.B. Martins, J. Ribeiro-Filho, F.R.A.S. Cesário, F.F. e Castro, T.R. de Albuquerque, M.N.M. Fernandes, B.A.F. da Silva, L.J. Quintans Júnior, A.A. de S. Araújo, P. dos P. Menezes, P.S. Nunes, I.G. Matos, H.D.M. Coutinho, A. Goncalves Wanderley, I.R.A. de Menezes, Anti-inflammatory activity of the essential oil obtained from Ocimum basilicum complexed with β-cyclodextrin (β-CD) in mice, Food and Chemical Toxicology 109 (2017) 836–846. https://doi.org/10.1016/j.fct.2017.02.027.
32. Marques CS, Carvalho SG, Bertoli LD, Villanova JCO, Pinheiro PF, dos Santos DCM, Yoshida MI, de Freitas JCC, Cipriano DF, Bernardes PC. β-Cyclodextrin inclusion complexes with essential oils: Obtention, characterization, antimicrobial activity and potential application for food preservative sachets. Food Res Int. 2019;119:499–509. https://doi.org/10.1016/j.foodres.2019.01.016.
33. Najafian S. Storage conditions affect the essential oil composition of cultivated Balm Mint Herb (Lamiaceae) in Iran. Ind Crops Prod. 2014;52:575–81. https://doi.org/10.1016/j.indcrop.2013.11.015.
34. Odak I, Škorić I, Talić S, Škobić D. Thermal Stability and Photostability of Satureja montana and Lavandula angustifolia Essential Oils. J Brazilian Chem Soc. 2021. https://doi.org/10.21577/0103-5053.20210099.